Mem. S.A.It. Vol. 93, 177

Memorie della

Inverse Compton halos around Pulsar Wind Nebulae

Fiorenza Donato and Sarah Recchia[1,2]

[1] Department of Physics, University of Torino, via P. Giuria, 1, 10125 Torino, Italy
[2] Istituto Nazionale di Fisica Nucleare, via P. Giuria, 1, 10125 Torino, Italy, e-mail: donato@to.infn.it

Received: 19 december 2021; Accepted: 21 June 2022

Abstract. The extended multi-TeV gamma-ray halos detected around pulsar wind nebulae, such as Geminga, Monogem (HAWC collaboration) and PSR J0622+3749 (LHAASO collaboration), are likely the result of inverse Compton scattering of runaway very high energy electrons and positrons released by the pulsar. Such halos provide a unique insight into the transport properties of very high energy cosmic rays in the turbulent interstellar medium. Such emission have been mostly analyzed in the assumption that cosmic rays undergo a pure isotropic diffusion, which lead to the surprising conclusion that the diffusion coefficient in the pulsars region should be at least two orders of magnitude smaller compared to nominal values found in models of Galactic cosmic ray propagation. On the other hand, just after injection from the source, particles rather propagate ballistically and only after a few scattering times the propagation becomes diffusive. We showed that when the transition from the ballistic to the diffusive regime is taken into account, the HAWC and LHAASO data can be reproduced with typical values of the interstellar diffusion coefficient.

Key words. ISM: cosmic rays – Gamma rays: observations – Stars: pulsars: general

1. Introduction

Extended gamma-ray halos around pulsar wind nebulae (PWNe) have been predicted many years ago (Aharonian 2004), and have been detected with unprecedented precision by the HAWC collaboration, around the Geminga and Monogem pulsars (Abeysekara et al. 2017) and, very recently, by the LHAASO experiment also, around the pulsar PSR J0622+3749 (Aharonian et al. 2021). Such structures are likely the result of inverse Compton scattering (ICS) on the interstellar radiation filed of very high energy electrons and positrons ($e^{\pm}$) accelerated at the pulsar's wind termination shock and diffusing in the source region.

ICS gamma-ray halos around pulsars have been mostly analyzed in the assumption that $e^{\pm}$ undergo a isotropic diffusive propagation around the source at any time-scale after being released. From such assumption, in order to explain the spatial extension of the gamma-ray halos (a few tens pc from the pulsar) the inferred cosmic ray (CR) diffusion coefficient in the PWNe region is at least two orders of magnitude smaller Abeysekara et al. (2017); Hooper et al. (2017); Tang & Piran (2019); Fang et al. (2018); Di Mauro et al. (2019, 2020); Giacinti et al. (2020) than the typical

values inferred from models of Galactic CR propagation (Strong et al. 2007). This result was quite surprising and, since then, no fully convincing explanation has been put forward (see e.g. López-Coto & Giacinti (2018); Evoli et al. (2018); Liu et al. (2019)).

In this project (Recchia et al. 2021) we investigated the propagation of CRs in the pulsar region and proposed an alternative explanation of the extension of the detected gamma-ray halos. In particular, we showed that small inferred diffusion coefficient found in previous analyses is a consequence of the wrong assumption that the CR propagation can be describes as diffusive at any time after injection from the source. In fact, just after injection particles rather propagate ballistically, and only after multiple scatterings in the turbulent interstellar medium (after a few scattering times) their motion becomes diffusive (Aloisio & Berezinsky 2005; Prosekin et al. 2015). Since pulsars release $e^{\pm}$ continuously, at any moment there will be particles whose motion has been isotropized (diffusive regime) and particles injected very recently that are not yet diffusing. We showed that, when the transition between the ballistic and diffusive regimes is taken into account, it is possible to fit the HAWC data for Geminga and Monogem, and the LHAASO data for PSR J0622+3749 with typical values of the interstellar CR diffusion coefficient.

2. Ballistic-diffusive propagation transition

The diffusion of CRs with the energy dependent diffusion coefficient $D(E)$ is characterized by the scattering time $\tau_c(E) = 3D(E)/c^2$ and mean free path $\lambda_c(E) = \tau_c\, c$ (see e.g. Strong et al. (2007)). The transport after injection from the source is characterized by three different phases: i) ballistic propagation for $t \ll \tau_c$; ii) diffusive transport (where the particle direction is isotropized) for $t > \tau_c$; iii) a transition between the two regimes called *quasi-ballistic* (see e.g Aloisio & Berezinsky (2005); Prosekin et al. (2015) and references therein). The application of the diffusive model to time-scales below τ_c wrongly results in a superluminal propagation (Aloisio & Berezinsky 2005; Prosekin et al. 2015).

The standard Galactic CR diffusion coefficient is given by $D(E) \approx D_0 E^{\delta}_{\rm GeV}$ where $E_{\rm GeV}$ is the particle energy in GeV, $D_0 \sim 1 - 4 \times 10^{28}{\rm cm}^2/{\rm s}$ and $\delta \sim 0.3 - 0.6$ (Strong et al. 2007). Notice that the mean free path λ_c increases with both D_0 and the particle energy. The $e^{\pm}$ responsible for the $\gamma-$ray emission detected by HAWC and LHAASO are mainly in the energy range 20 – 200 TeV (see Di Mauro et al. (2021)), which corresponds to a $\lambda_c \gtrsim 3-30$ pc in the standard Galactic diffusion coefficient. The spatial extension of $\approx$ 10 pc measured for the γ-ray halo around Geminga, Monogem and PSR J0622+3749 (Abeysekara et al. 2017; Aharonian et al. 2021) is comparable to these values for the mean free path.

The injection and propagation of $e^{\pm}$ in the pulsar region, for a source that turned on at time t=0 and with age T, is treated as follows (see Recchia et al. (2021) and references therein for details): i) particles are assumed to be injected with a power-law plus exponential cut-off spectrum, $Q(E)$, and with a time-dependent luminosity that reflects the pulsar spin-down luminosity $L(t) = \eta L_0 \left(1 + \frac{t}{\tau_0}\right)^{(-(n+1)/(n-1))}$. Here L_0 is the initial spin-down luminosity, n is the braking index (assumed to be 3) and τ_0 (order of a few kyrs) is the typical pulsar spin down timescale, η is the $e^{\pm}$ conversion efficiency; ii) the propagation of particle injected at times $T - \tau_c < t_0 \leq T$ is treated in the ballistic regime (particles move spherically at roughly the speed of light), and the resulting distribution function at distance r from the source reads:

$$f_{ball}(r, E) = \frac{Q(E)L(T)}{4\pi c r^2} H(\tau_c\, c - r) \qquad (1)$$

where $H(\tau_c\, c - r)$ is the Heaviside function. Here we neglected energy losses (the loss time is much longer than τ_c in the relevant energy range) and assumed that the pulsar luminosity is constant during τ_c ($\tau_c \ll \tau_0$, few kys against few tens yrs); iii) particles injected at times $t_0 \leq T - \tau_c$ are treated in the diffusive regime,

with the inclusion of energy losses. The particle distribution function reads:

$$f_{\rm diff}(r,E) = \int_0^{T-\tau_c} dt_0 \frac{Q(E_0)L(t_0)}{\pi^{3/2} r_d^3(E,E_0)} \frac{b(E_0)}{b(E)} e^{-\frac{r^2}{r_d^2}} \quad (2)$$

where $b(E) = dE/dt$ is the energy loss rate, which includes ICS losses on the interstellar radiation field (see Di Mauro et al. (2021) for details) and synchrotron radiation losses assuming a Galactic magnetic field of $3\,\mu$G. Due to losses, particles emitted at time t_0 with energy E_0 cool down to energy E during the time $T - t_0$, and $r_d^2(E,E_0) = 4\int_E^{E_0} D(E')/b(E')dE'$ is the propagation length squared; iv) The total $e^\pm$ density is given by $f_e(r,E) = f_{\rm ball}(r,E) + f_{\rm diff}(r,E)$. Moreover, following the prescription proposed by Prosekin et al. (2015), we took into account the anisotropic angular distribution of $e^\pm$ in the ballistic and quasi-ballistic regime, which affects the size of the detected gamma-ray halo. Indeed, since in the ICS process photons are emitted mainly along the direction of the parent particle, in the diffusive regime the $e^\pm$ distribution is isotropic and the size of the $\gamma-$ray halo reflects the size of the $e^\pm$ halo, while in the strictly ballistic regime the $\gamma-$ray source would be detected as point-like (Gabici & Aharonian 2005; Prosekin et al. 2015).

We showed that, for typical pulsar parameters, the gamma-ray spatial profile of the multi-TeV ICS halos is dominated, up to a distance $d \approx \lambda_c(E)/3$ from the source, by $e^\pm$ injected very recently, namely within the last τ_c, and that move quasi-ballistically. The resulting spatial profile is a bit steeper than $\propto 1/r$. At larger distances the gamma-ray profile is dominated by particles injected earlier that propagate diffusively, which gives a rather flat profile up to a distance $d \approx r_d \sim \sqrt{4\,D(E)\,t_{\rm loss}(E)}$, where $t_{\rm loss}$ is the time scale for energy losses. Beyond that distance particles have lost all their energy, which gives a cut-off on the gamma-ray profile.

The transition point between ballistic and diffusive regime is regulated by the normalization of the diffusion coefficients and by the particle energy. For $D_0 \lesssim 10^{27}\,{\rm cm}^2/{\rm s}$ the transition would happen very close to the source ($d < 1$ pc, and a typical bow-shock size of $\lesssim 1$ pc) and the extension of the three examined gamma-ray halos would be rather connected to the particles diffusion-loss length. Instead, for $D_0 = 10^{28} - 10^{29}\,{\rm cm}^2/{\rm s}$, $\lambda_c > 10$ pc in the relevant energy range and the spatial extension of the $\gamma-$ray halo is substantially determined by the quasi-ballistic propagation regime.

3. Results

We applied the ballistic-diffusive model to fit the HAWC data for the surface brightness of Geminga and Monogem and the LHAASO data for PSR J0622+3749, taking the the normalization of the diffusion coefficient D_0 and the $e^\pm$ conversion efficiency η as free parameters. Our benchmark values for the other relevant parameters are reported in Table. 1. In Fig. 1 we compare our prediction with the HAWC and LHAASO data.

For all three sources the χ^2 as a function of D_0 exhibits two minima, one at low $D_0 \approx 10^{25}\,{\rm cm}^2/{\rm s}$ and one at values of $D_0 \approx 10^{28}\,{\rm cm}^2/{\rm s}$ typically found in Galactic CR propagation models. The first minimum corresponds to the case, also found in previous analyses, where the diffusion coefficient is strongly suppressed and the extension of the $\gamma-$ray halo is linked to the diffusion-loss length $r_d \sim \sqrt{4\,D\,t_{\rm loss}}$. In this scenario the $\gamma-$ray morphology is influenced by the exponential cut-off $\exp(-r^2/r_d^2)$ that appears in the diffusive solution. The second minimum corresponds to a scenario where the ballistic-diffusive transition takes place at a few tens of parsec from the source, and the surface brightness is shaped by such transition.

The best-fit efficiency in the two cases is very different, $\lesssim 10\%$ in the suppressed diffusion scenario, close to $\approx 100\%$ ballistic-diffusive scenario. On the other hand, large conversion efficiencies are expected in pulsars and such estimates probably represents an upper limit (see discussion by Recchia et al. (2021)).

Table 1. Characteristics of Geminga, Monogem and PSR J0622+3749 and injection spectrum parameters: $\dot{E}$ is the current spin-down luminosity, T is the age, l the distance from Earth, τ_0 the assumed spin-down timescale and n the braking index, E_c the cut-off energy.

	$\dot{E}$ [erg/s]	T [kyr]	l [kpc]	τ_0 [kyr]	n
Geminga	3.25×10^{34}	342	0.19	12.0	3
Monogem	3.8×10^{34}	111	0.288	12.0	3
PSR J0622+3749	2.7×10^{34}	208	1.6	12.0	3
Injection Spectrum	spectral index			E_c	
	1.5			150 TeV	

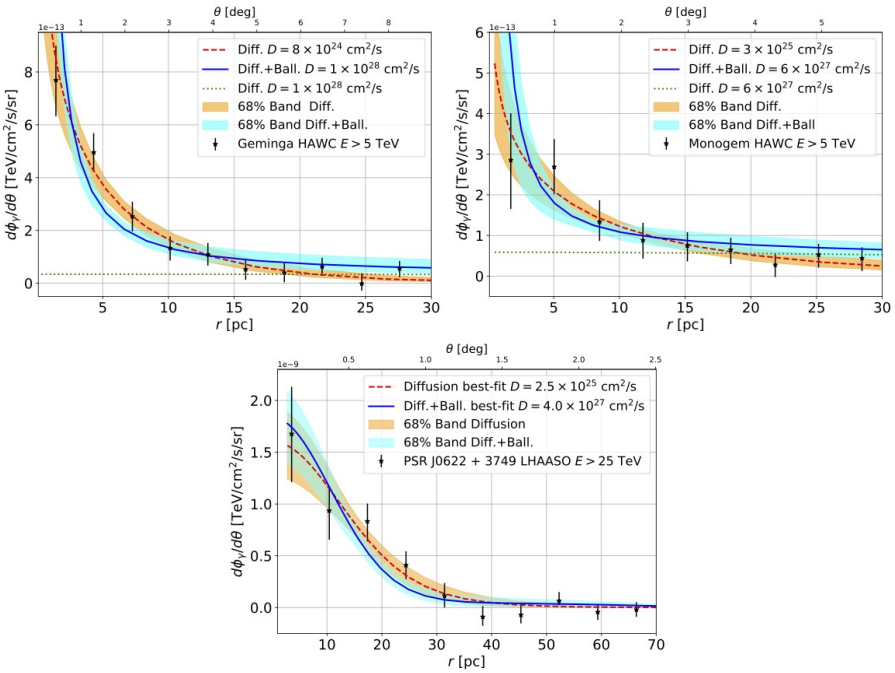

Fig. 1. Fit to the HAWC data for Geminga (top left panel) and Monogem (top right panel), and to the PSR J0622+3749 (bottom panel) in the diffusive regime (red dotted line) and in the combined diffusive and ballistic model (blue solid line and cyan band).

4. Other studies on the origin of cosmic rays and on the cosmic ray propagation

During the project *Inverse Compton halos around Pulsar Wind Nebulae*, we also investigated other aspects related to the origin of CRs and to the CR transport.

The problem of the escape of CRs from sources and their propagation in the source region has been studied also in the case of protons and heavier nuclei released by supernova remnants (Recchia et al. 2021b). In this work we estimated the amount of grammage that CRs may accumulate in the source region. The work was motivated by alternative CR propagation scenarios in which CRs secondaries (including positrons and antiprotons) are not only produced during the CR propagation in the Galaxy, but also within or nearby CR accelerators.

We also investigated the possible origin of the giant ($\sim$ 100 kpc scale) gamma-ray halo

recently detected by *Fermi*-LAT around the Adromeda Galaxy (Recchia et al. 2021a). We showed that such halo may be produced by a giant CR halo surrounding that galaxy and could be both of hadronic (interaction of CR protons with the gas) and leptonic origin (ICS of electrons). We investigated in which scenarios the existence of such particle halos is possible and showed that, in the hadronic scenario, if the Milky Way hosts a halo similar to that of Andromeda, it could be possible to explain the isotropic neutrino flux detected by IceCube up to PeV energies.

Finally, we collaborated to the study of the phases of the interstellar medium from which CRs are mostly accelerated as based on their composition (Tatischeff et al. 2021), and to the impact of stocastic fluctuations of sub-GeV CRs in the formation of the low-energy CR spectrum detected by Voyager (Phan et al. 2021).

5. Conclusions

In this project we showed that, contrary to the established consensus, the HAWC data for Geminga and Monogem, and the LHAASO data PSR J0622+3749, do not necessarily require a suppressed diffusion coefficient (difficult to justify theoretically) in the source region compared to typical values of the interstellar CR diffusion coefficient. Instead, when the ballistic-diffusive propagation transition is taken into account, it is possible to fit such data with typical values of the diffusion coefficient used to fit other CR data.

During the project, we also investigated the transport of CRs in the source region also in the case of supernova remnants and the formation of giant CR halos in galaxies. Finally, we also contributed to the study of the Galactic CR composition and of the possible interpretation of the low energy CR spectra detected by Voyager.

References

Abeysekara, A. U. et al. 2017, Science, 358, 911

Aharonian, F. et al. 2021, Phys. Rev. Lett., 126, 241103

Aharonian, F. A. 2004, Very high energy cosmic gamma radiation : a crucial window on the extreme Universe (WORLD SCIENTIFIC)

Aloisio, R. & Berezinsky, V. S. 2005, ApJ, 625, 249

Di Mauro, M., Donato, F., & Manconi, S. 2021, Phys. Rev. D, 104, 083012

Di Mauro, M., Manconi, S., & Donato, F. 2019, Phys. Rev. D, 100, 123015

Di Mauro, M., Manconi, S., & Donato, F. 2020, Phys. Rev. D, 101, 103035

Evoli, C., Linden, T., & Morlino, G. 2018, Phys. Rev. D, 98, 063017

Fang, K., Bi, X.-J., Yin, P.-F., & Yuan, Q. 2018, Astrophys. J., 863, 30

Gabici, S. & Aharonian, F. A. 2005, Phys. Rev. Lett., 95, 251102

Giacinti, G., Mitchell, A. M. W., López-Coto, R., et al. 2020, Astron. Astrophys., 636, A113

Hooper, D., Cholis, I., Linden, T., & Fang, K. 2017, Phys. Rev. D, 96, 103013

Liu, R.-Y., Yan, H., & Zhang, H. 2019, Phys. Rev. Lett., 123, 221103

López-Coto, R. & Giacinti, G. 2018, Mon. Not. Roy. Astron. Soc., 479, 4526

Phan, V. H. M., Schulze, F., Mertsch, P., Recchia, S., & Gabici, S. 2021, Phys. Rev. Lett., 127, 141101

Prosekin, A. Y., Kelner, S. R., & Aharonian, F. A. 2015, Phys. Rev. D, 92, 083003

Recchia, S., Di Mauro, M., Aharonian, F. A., et al. 2021, Phys. Rev. D, 104, 123017

Recchia, S., Gabici, S., Aharonian, F. A., & Niro, V. 2021a, ApJ, 914, 135

Recchia, S., Galli, D., Nava, L., et al. 2021b, arXiv e-prints, arXiv:2106.04948

Strong, A. W., Moskalenko, I. V., & Ptuskin, V. S. 2007, Annual Review of Nuclear and Particle Science, 57, 285

Tang, X. & Piran, T. 2019, Mon. Not. Roy. Astron. Soc., 484, 3491

Tatischeff, V., Raymond, J. C., Duprat, J., Gabici, S., & Recchia, S. 2021, MNRAS, 508, 1321